Acta Crystallographica Section C
Crystal Structure Communications
ISSN 0108-2701

Channel-forming solvates of 6-chloro-2,5-dihydroxypyridine and its solvent-free tautomer 6-chloro-5-hydroxy-2-pyridone

Sean R. Parkin[a]* and Edward J. Behrman[b]

[a]Department of Chemistry, University of Kentucky, Lexington, KY 40506-0055, USA, and [b]Department of Biochemistry, Ohio State University, Columbus, OH 43210, USA
Correspondence e-mail: s.parkin@uky.edu

Received 20 July 2009
Accepted 9 September 2009
Online 30 September 2009

On crystallization from $CHCl_3$, CCl_4, CH_2ClCH_2Cl and $CHCl_2$-$CHCl_2$, 6-chloro-5-hydroxy-2-pyridone, $C_5H_4ClNO_2$, (I), undergoes a tautomeric rearrangement to 6-chloro-2,5-dihydroxypyridine, (II). The resulting crystals, *viz.* 6-chloro-2,5-dihydroxypyridine chloroform 0.125-solvate, $C_5H_4ClNO_2{\cdot}0.125CHCl_3$, (II*a*), 6-chloro-2,5-dihydroxypyridine carbon tetrachloride 0.125-solvate, $C_5H_4ClNO_2{\cdot}0.125CCl_4$, (II*b*), 6-chloro-2,5-dihydroxypyridine 1,2-dichloroethane solvate, $C_5H_4ClNO_2{\cdot}C_2H_4Cl_2$, (II*c*), and 6-chloro-2,5-dihydroxypyridine 1,1,2,2-tetrachloroethane solvate, $C_5H_4ClNO_2{\cdot}C_2H_2Cl_4$, (II*d*), have $I4_1/a$ symmetry, and incorporate extensively disordered solvent in channels that run the length of the *c* axis. Upon gentle heating to 378 K *in vacuo*, these crystals sublime to form solvent-free crystals with $P2_1/n$ symmetry that are exclusively the pyridone tautomer, (I). In these sublimed pyridone crystals, inversion-related molecules form $R_2^2(8)$ dimers *via* pairs of N—H···O hydrogen bonds. The dimers are linked by O—H···O hydrogen bonds into $R_6^4(28)$ motifs, which join to form pleated sheets that stack along the *a* axis. In the channel-containing pyridine solvate crystals, *viz.* (II*a*)–(II*d*), two independent host molecules form an $R_2^2(8)$ dimer *via* a pair of O—H···N hydrogen bonds. One molecule is further linked by O—H···O hydrogen bonds to two 4_1 screw-related equivalents to form a helical motif parallel to the *c* axis. The other independent molecule is O—H···O hydrogen bonded to two $\overline{4}$ related equivalents to form tetrameric $R_4^4(28)$ rings. The dimers are π–π stacked with inversion-related dimers, which in turn stack the $R_4^4(28)$ rings along *c* to form continuous solvent-accessible channels. $CHCl_3$, CCl_4, CH_2ClCH_2Cl and $CHCl_2CHCl_2$ solvent molecules are able to occupy these channels but are disordered by virtue of the $\overline{4}$ site symmetry within the channels.

Comment

6-Chloro-5-hydroxy-2-pyridone, (I), was synthesized as part of a study of the Elbs oxidation of 2-pyridones (Behrman, 2008). The crude material contains some of the *o*-isomer, 6-chloro-2,3-dihydroxypyridine, but that can be removed by recrystallization from $CHCl_3$. Elemental analysis of the crystals and their ^{1}H NMR spectra showed the presence of approximately one $CHCl_3$ guest for every eight of the pyridine host – an unusual ratio. Some small molecules are known to form large-diameter channels *via* elaborate hydrogen-bonding networks (see, for example, Glidewell *et al.*, 2005; Hao *et al.*, 2005), and this seemed a likely cause of the unusual guest–host ratio. Given the considerable current interest in crystal engineering, the potential applications of large solvent-accessible channels (Sisson *et al.*, 2005; Maly *et al.*, 2007; Comotti *et al.*, 2009; Furukawa & Yaghi, 2009) and the influence of substituents at the 6-position on tautomerism in 2-pyridones (Almlöf *et al.*, 1971; Kvick, 1976; Johnson, 1984), we undertook a study of (I) crystallized from a series of solvents. We report here the structure of the pyridine tautomer, 6-chloro-2,5-dihydroxypyridine, (II), as the chloroform solvate, (II*a*), and the carbon tetrachloride solvate, (II*b*). Solvate crystals grown from CH_2ClCH_2Cl, (II*c*), and $CHCl_2CHCl_2$, (II*d*), were also obtained. Although the host-molecule framework is ostensibly the same in all four solvates, the disorder of the solvent was too severe in (II*c*) and (II*d*) to be modelled in an acceptable way. Refined models of (II*c*) and (II*d*) in which the solvent contribution was removed using SQUEEZE (*PLATON*; Spek, 2009) are given in the *Supplementary Material*. In addition to the low-temperature structures, room temperature structure determinations of (I) and (II*d*) were also performed. There were no substantive differences between these room-temperature structures and their low-temperature counterparts, other than the expected difference in volume, which was *ca* 2–3%, as is common for molecular crystals. Data for (I), (II*a*) and (II*b*) are included here, and full details of (II*c*), (II*d*), (IRT) and (II*d*RT) are available in the *Supplementary Material*.

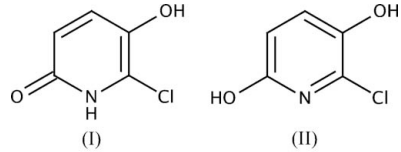

(I) (II)

(II*a*) = (II)·0.125$CHCl_3$
(II*b*) = (II)·0.125CCl_4

Attempts to anneal the disordered solvent or to drive the solvent from the channels at elevated temperatures (above *ca* 378 K) led to the collapse of the host framework and to sublimation growth of solvent-free crystals of the pyridone tautomer, (I) (Fig. 1). Bond lengths and angles in (I) (Table 1) are within the normal range (Allen *et al.*, 1987). In these sublimed crystals, inversion-related molecules form $R_2^2(8)$ dimers (Bernstein *et al.*, 1995) *via* pairs of N—H···O hydrogen bonds. Four such dimers are linked by O—H···O hydrogen bonds into $R_6^4(28)$ motifs, which combine to form extensive pleated sheets (Fig. 2) that stack along the *a* axis. Hydrogen-bond parameters for (I) are given in Table 2.

Compounds (II*a*)–(II*d*) are isostructural with regard to the host-molecule framework. The following description is based

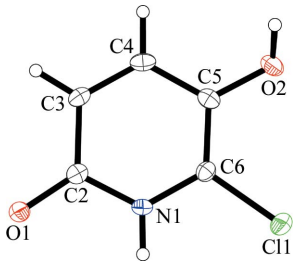

Figure 1
The molecular structure of (I), showing the atom-numbering scheme. Displacememt ellipsoids are drawn at the 50% probability level and H atoms are shown as small spheres of arbitrary radii.

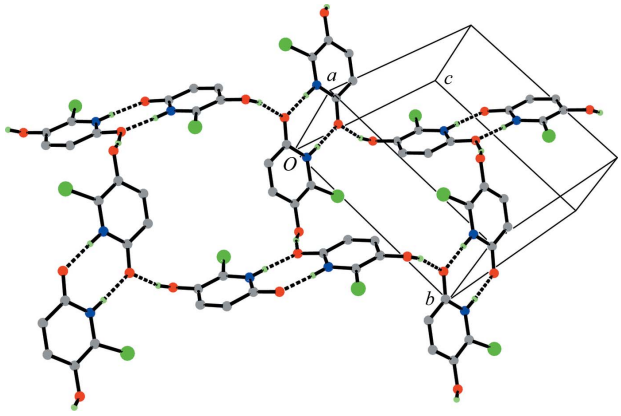

Figure 2
The hydrogen bonding in (I). The molecules form $R_2^2(8)$ dimers *via* pairs of N—H···O hydrogen bonds, and these are in turn linked *via* four sets of O—H···O hydrogen bonds to form $R_6^4(28)$ motifs which, together with the dimers, create pleated layers. Hydrogen bonds are represented by dashed lines.

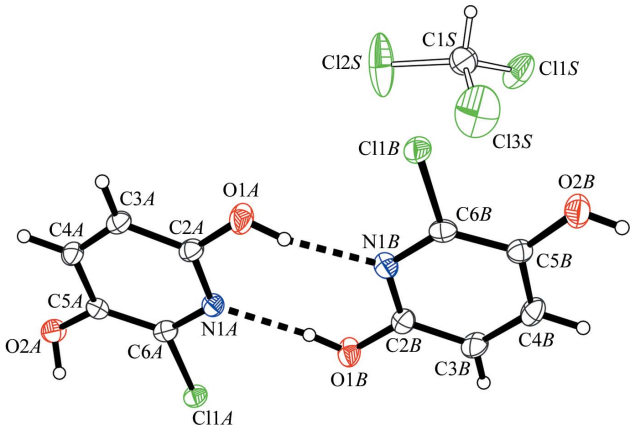

Figure 3
The asymmetric unit of chloroform solvate (II*a*), showing the atom-numbering scheme and the dimerization of the host molecules *via* hydrogen bonding (dashed lines). Displacement ellipsoids are drawn at the 50% probability level and H atoms are shown as small spheres of arbitrary radii. The chloroform guest molecule sits on a site of $\overline{4}$ symmetry and is thus extensively disordered. The structures of the CCl_4, CH_2ClCH_2Cl and $CHCl_2CHCl_2$ solvates, *viz.* (II*b*), (II*c*) and (II*d*), respectively, are ostensibly the same, but the guest solvents in (II*c*) and (II*d*) were too badly disordered to model.

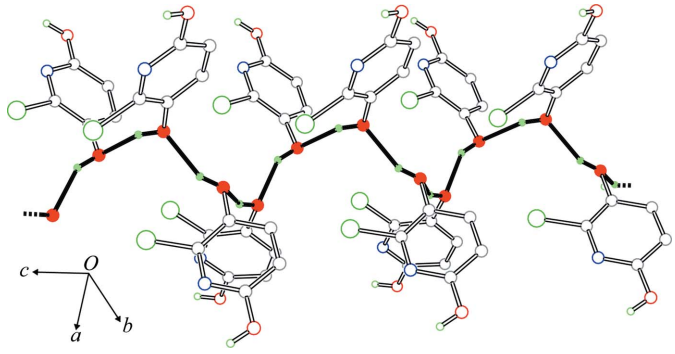

Figure 4
Three turns of an extended hydrogen-bonded helix motif in (II*a*), viewed perpendicular to the *c* axis. This helix propagates along the 4_1 screw axis, parallel to the crystallographic *c* axis, and includes only molecules of type *A* (Fig. 3). The CCl_4, CH_2ClCH_2Cl and $CHCl_2CHCl_2$ solvates, *viz.* (II*b*), (II*c*) and (II*d*), respectively, all have essentially the same structural feature. Bonds and atoms involved in the helix are drawn with solid colours. Dashed lines indicate continuation of the helix.

upon the structure of (II*a*), but unless stated otherwise the general features apply to all four solvates. Bond lengths and angles (Table 3) in the two independent molecules (designated with suffixes *A* and *B* in Fig. 3) are normal, and the molecules are largely flat [r.m.s. deviations from planarity = 0.027 (2) and 0.009 (2) Å, respectively, for all non-H atoms of molecules *A* and *B*]. Indeed, the only significant deviation from planarity is for atom H1*A*, which is almost *syn* with respect to the O1*A*—H1*A* hydroxy group *para* to it, but twisted out of the plane of the ring by about 39°. This is a consequence of intermolecular hydrogen bonding of molecule *A* in a repeating *C*(2) chain motif to 4_1 screw-related equivalents, to form helices that propagate along *c* (Fig. 4). In molecule *B*, the corresponding torsion angle is only 4° out of planarity and so strictly *anti* with respect to O2*B*—H2*B*. The *B* molecules are linked by O—H···O hydrogen bonds to $\overline{4}$ related equivalents to form large tetrameric $R_4^4(28)$ rings (Fig. 5). The two independent molecules (*A* helix-forming and *B* ring-forming) are linked in a pseudo-inversion-related manner into planar $R_2^2(8)$ dimers by pairs of hydrogen bonds (O2*A*—H2*A*···N1*B* and O2*B*—H2*B*···N1*A*). These dimers are π–π stacked with inversion-related dimers [mean π–π spacing = 3.351 (3) Å], with concomitant stacking of the $R_4^4(28)$ rings along the *c* axis to form continuous solvent-accessible channels (Fig. 6). Solvent molecules of appropriate size (*e.g.* $CHCl_3$, CCl_4, CH_2ClCH_2Cl and $CHCl_2CHCl_2$) are able to occupy the channels, but are disordered as a consequence of the $\overline{4}$ symmetry. Crystals grown from either acetone or propan-2-ol were too small for conventional X-ray analysis, but gave ^{1}H NMR spectra that suggested similar stoichiometry to (II*a*)–(II*d*). Larger solvent molecules, such as chlorobenzene, gave tiny crystals that were far too small for diffraction studies, but that gave IR spectra identical to the sublimate, as distinct from the IR spectra of the solvated crystals.

We anticipated that since CCl_4 is tetrahedral it might occupy the channels in an ordered fashion, but this was not the case. Indeed, it is the nature of the solvent within these solvate crystals that causes the most significant (albeit small) differences between them. Channel volumes differ slightly owing to the need to accomodate solvent molecules of different size.

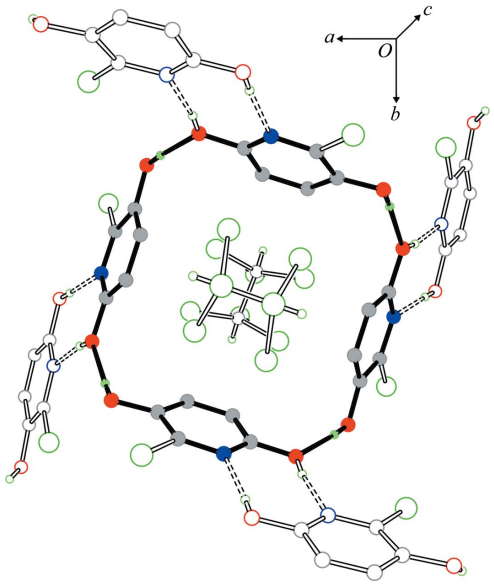

Figure 5
One of the large $R_4^4(28)$ O—H···O hydrogen-bonded rings in (II*a*), viewed perpendicular to the *bc* plane. Atoms and bonds involved in the large rings are drawn with solid colours. Dashed lines represent O—H···N hydrogen bonds within $R_2^2(8)$ dimer pairs between molecules of type *A* (helix-forming) and type *B* (ring-forming). These ring structures stack along the *c* direction to form solvent-accessible channels. A disordered $CHCl_3$ molecule is shown within the cavity.

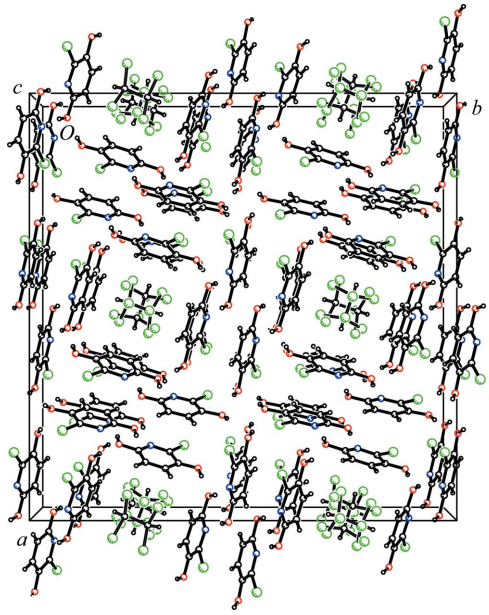

Figure 6
A packing diagram for (II*a*), viewed perpendicular to the *bc* plane, showing the presence of disordered guest solvent molecules within channels parallel to *c*. Crystals of (II*b*), (II*c*) and (II*d*) exhibit essentially identical packing.

Estimates of channel volume per unit cell using *PLATON* (Spek, 2009) were 186.0, 187.5, 185.9 and 198.6 Å^3 for (II*a*), (II*b*), (II*c*) and (II*d*), respectively, at 90 K. For structures (II*a*) and (II*b*) it proved possible to model $CHCl_3$ and CCl_4 solvent molecules disordered on the $\overline{4}$ of Wyckoff site *a* in $I4_1/a$, such that the site is fully occupied overall. For (II*c*) and (II*d*), although no satisfactory disorder model could be found, an estimate of the occupancy of the solvent channels was made *via* the electron count of the SQUEEZE routine in *PLATON*. To within a few percent, the $\overline{4}$ sites in each of (II*a*)–(II*d*) appear to be fully occupied, giving a solvent–host ratio of 1:8. Alternative estimates based on NMR spectroscopy [600 MHz ^{1}H NMR for (II*a*), (II*c*) and (II*d*); 800 MHz ^{13}C NMR for (II*b*)] were less clear cut [1:8, 1:7, 1:12, 1:10.5 for (II*a*), (II*b*), (II*c*) and (II*d*), respectively], but the sample treatment was necessarily very different for the NMR experiments.

Johnson (1984) gives a comprehensive summary of the factors which influence the tautomeric ratio for the 2-pyridone/2-hydroxypyridine system. Whereas the pyridone form predominates in the parent compound, a 6-chloro substituent shifts the equilibrium toward the hydroxy form, both in solution and in the gas phase. Thus, changes in molecular environment within a crystal structure can easily favour one form or the other. In the present case, differences between the molecular structures of (I) and (II*a*) (Tables 1 and 3) are largely as expected for pyridone–pyridine tautomerism. The C2—O1 carbonyl bond in (I) lengthens from 1.277 (2) Å upon hydrogen shift to 1.338 (2) and 1.348 (3) Å, respectively, for the hydroxy groups of molecules *A* and *B* in (II*b*). The lack of aromaticity in (I) is clearly evident in the alternation of C—C bond lengths around the ring, while the aromaticity in (II) is well displayed by the similarity in the C—C bond lengths. Although the $R_2^2(8)$ dimers in (I) and in (II*a*)–(II*d*) are superficially similar in appearance, in (I) the pairs of hydrogen bonds are N—H···O interactions between molecules related by crystallographic inversion, while in (II*a*)–(II*d*) they are O—H···N interactions and each molecule of the dimer is crystallographically unique. Average donor–acceptor distances within these dimers are slightly shorter for O—H···N at 2.716 (8) Å (for the eight hydrogen bonds of this type in the four pyridine structures), compared with the pyridone N—H···O distance of 2.7393 (18) Å in (I). The O—H···O donor–acceptor distances that link dimers in pyridines (II*a*)–(II*d*) [average 2.734 (10) Å for four such hydrogen bonds], where the acceptor is a hydroxy O atom, are considerably longer than that in (I) [2.6507 (17) Å], where the acceptor is a carbonyl O atom.

Experimental

The synthesis of (I) has been described previously (Behrman, 2008). Crystals suitable for X-ray diffraction analysis of each of the solvates were prepared as follows. For (II*a*), from $CHCl_3$, the crude material (200 mg) was dissolved in hot $CHCl_3$ (9 ml). For (II*b*), from CCl_4, $CHCl_3$-containing crystals (25 mg) were dissolved in boiling CCl_4 (25 ml). For (II*c*), from CH_2ClCH_2Cl, $CHCl_3$-containing crystals (200 mg) were dissolved in boiling CH_2ClCH_2Cl (10 ml). For (II*d*), from $CHCl_2CHCl_2$, $CHCl_3$-containing crystals (50 mg) were dissolved in hot (not boiling) $CHCl_2CHCl_2$ (2.5 ml). In each case, crystals grew on cooling as pale-yellow needles. Small crystals of (I) formed on sublimation of the solvate crystals at 378 K and 0.5 mm Hg (1mm Hg = 133.322 Pa).

Crystals formed from all four solvents melt at 424–425 K (decomposition), as does the sublimate. This implies that solvent loss below the melting point occurs for all forms of (II), which then transform to (I), thereby yielding a single melting point. All solvate crystals give identical IR spectra as mulls in Nujol: 1668, 1605, 1491, 1325, 1283, 1240, 1208, 1182, 1085, 912, 811, 691 cm^{-1}. When these crystals are sublimed *in vacuo*, different IR spectra result: 1591, 1503, 1337, 1246, 1195, 1183, 1168, 1081, 910, 810, 693 cm^{-1}. UV [1×10^{-4} *M* aqueous HCl, λ_{max} (nm), ε (M^{-1} cm^{-1})]: 301, 4900; 222, 5100; 330–340 (*sh*). The sublimate gives 301, 5700; 222, 5550, 330–340 (*sh*). Crystallization from chlorobenzene gives material with the same IR spectrum as the sublimate. The ^{1}H NMR spectrum of the sublimate no longer shows evidence of solvent but is otherwise identical to that reported previously (Behrman, 2008). ^{1}H NMR spectra of crystals grown from either acetone or propan-2-ol suggested stoichiometry similar to (II*a*)–(II*d*), but the crystals were too small for X-ray analysis. Estimates of guest–host molecule ratios were made either by 600 MHz ^{1}H NMR [(II*a*), (II*c*) and (II*d*)] or by 800 MHz ^{13}C NMR with inverse gated ^{1}H decoupling and a delay time of 8 s under the following conditions: 18 mg crystals, 15 mg $Cr(acac)_3$, 0.6 ml $CDCl_3$, 0.3 ml DMSO-d_6 (Berger & Braun, 2004), as well as by disorder model refinement [(II*a*) and (II*b*)] and by a count of the number of electrons present within the channels of (II*a*)–(II*d*) using SQUEEZE in *PLATON* (Spek, 2009).

Compound (I)

Crystal data

$C_5H_4ClNO_2$
M_r = 145.54
Monoclinic, $P2_1/n$
a = 4.1960 (1) Å
b = 10.6058 (3) Å
c = 13.0059 (4) Å
β = 90.8559 (12)°
V = 578.72 (3) Å^3
Z = 4
Mo $K\alpha$ radiation
μ = 0.57 mm^{-1}
T = 90 K
0.15 × 0.15 × 0.12 mm

Data collection

Nonius KappaCCD area-detector diffractometer
7956 measured reflections
1329 independent reflections
1124 reflections with $I > 2\sigma(I)$
R_{int} = 0.037

Refinement

$R[F^2 > 2\sigma(F^2)]$ = 0.034
$wR(F^2)$ = 0.081
S = 1.12
1329 reflections
83 parameters
H-atom parameters constrained
$\Delta\rho_{max}$ = 0.28 e Å^{-3}
$\Delta\rho_{min}$ = −0.26 e Å^{-3}

Compound (II*a*)

Crystal data

$C_5H_4ClNO_2{\cdot}0.125CHCl_3$
M_r = 160.46
Tetragonal, $I4_1/a$
a = 27.1736 (10) Å
c = 6.9253 (2) Å
V = 5113.7 (3) Å^3
Z = 32
Mo $K\alpha$ radiation
μ = 0.68 mm^{-1}
T = 90 K
0.20 × 0.18 × 0.18 mm

Data collection

Nonius KappaCCD area-detector diffractometer
Absorption correction: multi-scan (*SCALEPACK*; Otwinowski & Minor, 1997)
T_{min} = 0.877, T_{max} = 0.888
12800 measured reflections
2924 independent reflections
1731 reflections with $I > 2\sigma(I)$
R_{int} = 0.069

Table 1
Selected geometric parameters (Å, °) for (I).

N1—C2	1.361 (2)	C4—C5	1.414 (2)
N1—C6	1.363 (2)	C5—O2	1.356 (2)
C2—O1	1.277 (2)	C5—C6	1.362 (2)
C2—C3	1.431 (2)	C6—Cl1	1.7162 (17)
C3—C4	1.356 (2)		
C2—N1—C6	123.64 (14)	O2—C5—C6	120.16 (16)
O1—C2—N1	119.31 (15)	O2—C5—C4	123.23 (15)
O1—C2—C3	124.95 (15)	C6—C5—C4	116.59 (16)
N1—C2—C3	115.74 (15)	C5—C6—N1	121.55 (16)
C4—C3—C2	120.48 (16)	C5—C6—Cl1	122.48 (14)
C3—C4—C5	121.98 (16)	N1—C6—Cl1	115.97 (12)

Table 2
Hydrogen-bond geometry (Å, °) for (I).

D—H···A	D—H	H···A	D···A	D—H···A
N1—H1···O1^{i}	0.88	1.86	2.7393 (18)	177
O2—H2···O1^{ii}	0.84	1.83	2.6507 (17)	166

Symmetry codes: (i) $-x+2, -y+1, -z+1$; (ii) $-x+\frac{3}{2}, y-\frac{1}{2}, -z+\frac{1}{2}$.

Refinement

$R[F^2 > 2\sigma(F^2)]$ = 0.052
$wR(F^2)$ = 0.146
S = 0.99
2924 reflections
198 parameters
12 restraints
H-atom parameters constrained
$\Delta\rho_{max}$ = 0.53 e Å^{-3}
$\Delta\rho_{min}$ = −0.44 e Å^{-3}

Compound (II*b*)

Crystal data

$C_5H_4ClNO_2{\cdot}0.125CCl_4$
M_r = 164.77
Tetragonal, $I4_1/a$
a = 27.1708 (4) Å
c = 6.9458 (1) Å
V = 5127.75 (13) Å^3
Z = 32
Cu $K\alpha$ radiation
μ = 6.62 mm^{-1}
T = 90 K
0.12 × 0.02 × 0.01 mm

Data collection

Bruker X8 Proteum diffractometer
Absorption correction: multi-scan (*SADABS* in *APEX2*; Bruker, 2006)
T_{min} = 0.672, T_{max} = 0.937
37025 measured reflections
2344 independent reflections
2237 reflections with $I > 2\sigma(I)$
R_{int} = 0.042

Refinement

$R[F^2 > 2\sigma(F^2)]$ = 0.034
$wR(F^2)$ = 0.092
S = 1.04
2344 reflections
223 parameters
63 restraints
H-atom parameters constrained
$\Delta\rho_{max}$ = 0.55 e Å^{-3}
$\Delta\rho_{min}$ = −0.81 e Å^{-3}

The H atoms in each of the structures were found in difference Fourier maps and subsequently placed in idealized positions, with C—H = 0.95 (C_{Ar}H) or 1.00 Å [in $CHCl_3$ of (II*a*)], N—H = 0.88 Å and O—H = 0.84 Å, and with U_{iso}(H) = 1.2U_{eq}(C,N) or 1.5U_{eq}(O).

In (II*a*) and (II*b*), the solvent molecules are disordered on sites of $\overline{4}$ point symmetry. They required restraints on interatomic distances (SADI in *SHELXL97*; Sheldrick, 2008) to maintain a chemically sensible geometry, and on displacement parameters (SIMU in *SHELXL97*) to counteract distortion of the resulting ellipsoids

Table 3
Selected geometric parameters (Å, °) for (II*a*).

N1*A*—C2*A*	1.333 (4)	N1*B*—C2*B*	1.333 (4)
N1*A*—C6*A*	1.340 (4)	N1*B*—C6*B*	1.334 (4)
C2*A*—O1*A*	1.343 (3)	C2*B*—O1*B*	1.355 (4)
C2*A*—C3*A*	1.391 (4)	C2*B*—C3*B*	1.390 (4)
C3*A*—C4*A*	1.373 (4)	C3*B*—C4*B*	1.370 (4)
C4*A*—C5*A*	1.397 (4)	C4*B*—C5*B*	1.399 (4)
C5*A*—C6*A*	1.366 (4)	C5*B*—O2*B*	1.351 (4)
C5*A*—O2*A*	1.375 (3)	C5*B*—C6*B*	1.376 (4)
C6*A*—Cl1*A*	1.738 (3)	C6*B*—Cl1*B*	1.740 (3)
C2*A*—N1*A*—C6*A*	117.9 (3)	C2*B*—N1*B*—C6*B*	117.7 (3)
N1*A*—C2*A*—O1*A*	119.0 (3)	N1*B*—C2*B*—O1*B*	117.7 (3)
N1*A*—C2*A*—C3*A*	122.7 (3)	N1*B*—C2*B*—C3*B*	122.5 (3)
O1*A*—C2*A*—C3*A*	118.2 (3)	O1*B*—C2*B*—C3*B*	119.9 (3)
C4*A*—C3*A*—C2*A*	118.1 (3)	C4*B*—C3*B*—C2*B*	118.6 (3)
C3*A*—C4*A*—C5*A*	120.0 (3)	C3*B*—C4*B*—C5*B*	120.2 (3)
C6*A*—C5*A*—O2*A*	124.8 (3)	O2*B*—C5*B*—C6*B*	118.9 (3)
C6*A*—C5*A*—C4*A*	117.4 (3)	O2*B*—C5*B*—C4*B*	124.8 (3)
O2*A*—C5*A*—C4*A*	117.7 (3)	C6*B*—C5*B*—C4*B*	116.3 (3)
N1*A*—C6*A*—C5*A*	123.9 (3)	N1*B*—C6*B*—C5*B*	124.8 (3)
N1*A*—C6*A*—Cl1*A*	116.1 (2)	N1*B*—C6*B*—Cl1*B*	116.0 (2)
C5*A*—C6*A*—Cl1*A*	120.0 (2)	C5*B*—C6*B*—Cl1*B*	119.2 (2)

Table 4
Hydrogen-bond geometry (Å, °) for (II*a*).

D—H···*A*	*D*—H	H···*A*	*D*···*A*	*D*—H···*A*
O1*A*—H1*A*···N1*B*	0.84	1.89	2.721 (3)	169
O2*A*—H2*A*···O2*A*^{i}	0.84	1.89	2.647 (2)	149
O1*B*—H1*B*···N1*A*	0.84	1.88	2.707 (3)	170
O2*B*—H2*B*···O1*B*^{ii}	0.84	1.89	2.723 (3)	174

Symmetry codes: (i) $-y+\frac{3}{4}, x+\frac{1}{4}, z+\frac{1}{4}$; (ii) $y+\frac{1}{4}, -x+\frac{3}{4}, -z+\frac{7}{4}$.

caused by the symmetry of the solvent site. In (II*b*), the CCl_4 was split over two sites, each with an occupancy of 0.125. The corresponding atoms in each fragment were close enough to warrant use of the EADP constraint in addition to SIMU. In (II*c*) and (II*d*), molecules of solvent were also disordered on sites of $\overline{4}$ symmetry, but suitable disorder models could not be found. In order to obtain a better quality refinement of the host-molecule framework, the SQUEEZE routine in *PLATON* (Spek, 2009) was used to remove the contribution from the disordered solvent.

Data collection: *COLLECT* (Nonius, 1998) for (I) and (II*a*); *APEX2* (Bruker, 2006) for (II*b*). Cell refinement: *SCALEPACK* (Otwinowski & Minor, 1997) for (I) and (II*a*); *APEX2* (Bruker, 2006) for (II*b*). Data reduction: *DENZO-SMN* (Otwinowski & Minor, 1997) for (I) and (II*a*); *APEX2* (Bruker, 2006) for (II*b*). For all three compounds, program(s) used to solve structure: *SHELXS97* (Sheldrick, 2008); program(s) used to refine structure: *SHELXL97* (Sheldrick, 2008); molecular graphics: *XP* in *SHELXTL* (Sheldrick, 2008); software used to prepare material for publication: *SHELXL97* (Sheldrick, 2008) and local procedures.

Table 5
Hydrogen-bond geometry (Å, °) for (II*b*).

D—H···*A*	*D*—H	H···*A*	*D*···*A*	*D*—H···*A*
O1*A*—H1*A*···N1*B*	0.84	1.89	2.726 (2)	172
O2*A*—H2*A*···O2*A*^{i}	0.84	1.90	2.6487 (15)	148
O1*B*—H1*B*···N1*A*	0.84	1.88	2.708 (2)	171
O2*B*—H2*B*···O1*B*^{ii}	0.84	1.91	2.738 (2)	168

Symmetry codes: (i) $-y+\frac{3}{4}, x+\frac{1}{4}, z+\frac{1}{4}$; (ii) $y+\frac{1}{4}, -x+\frac{3}{4}, -z+\frac{7}{4}$.

The authors are grateful to the late Dr Charles Cottrell for his NMR expertise, and to Professor Carol Brock for helpful discussions. X-ray data were collected at the University of Kentucky using both a Nonius KappaCCD diffractometer purchased with University funds and a Bruker Nonius X8 Proteum diffractometer obtained with funding from the NSF (MRI grant No. 0319176).

Supplementary data for this paper are available from the IUCr electronic archives (Reference: MX3019). Services for accessing these data are described at the back of the journal.

References

Allen, F. H., Kennard, O., Watson, D. G., Brammer, L., Orpen, A. G. & Taylor, R. (1987). *J. Chem. Soc. Perkin Trans. 2*, pp. S1–19.
Almlöf, J., Kvick, Å. & Olovsson, I. (1971). *Acta Cryst.* B**27**, 1201–1208.
Behrman, E. J. (2008). *Synth. Commun.* **38**, 1168–1175.
Berger, S. & Braun, S. (2004). *200 and More NMR Experiments*. Weinheim: Wiley–VCH.
Bernstein, J., Davis, R. E., Shimoni, L. & Chang, N.-L. (1995). *Angew. Chem. Int. Ed. Engl.* **34**, 1555–1573.
Bruker (2006). *APEX2*. Bruker AXS Inc., Madison, Wisconsin, USA.
Comotti, A., Bracco, S., Distefano, G. & Sozzani, P. (2009). *Chem. Commun.* pp. 284–286.
Furukawa, H. & Yaghi, O. M. (2009). *J. Am. Chem. Soc.* **131**, 8875–8883.
Glidewell, C., Low, J. N., Skakle, J. M. S. & Wardell, J. L. (2005). *Acta Cryst.* C**61**, o493–o495.
Hao, X., Parkin, S. & Brock, C. P. (2005). *Acta Cryst.* B**61**, 689–699.
Johnson, C. D. (1984). *Comprehensive Heterocyclic Chemistry*, Vol. 2, edited by A. R. Katritzky & C. W. Rees, pp. 148–157. Oxford: Pergamon.
Kvick, Å. (1976). *Acta Cryst.* B**32**, 220–224.
Maly, K. E., Gagnon, E., Maris, T. & Wuest, J. D. (2007). *J. Am. Chem. Soc.* **129**, 4306–4322.
Nonius (1998). *COLLECT*. Nonius BV, Delft, The Netherlands.
Otwinowski, Z. & Minor, W. (1997). *Methods in Enzymology*, Vol. 276, *Macromolecular Crystallography*, Part A, edited by C. W. Carter Jr & R. M. Sweet, pp. 307–326. New York: Academic Press.
Sheldrick, G. M. (2008). *Acta Cryst.* A**64**, 112–122.
Sisson, A. L., Sanchez, V. D. A., Magro, G., Griffin, A. M. E., Shah, S., Charmant, J. P. H. & Davis, A. P. (2005). *Angew. Chem. Int. Ed.* **44**, 6878–6881.
Spek, A. L. (2009). *Acta Cryst.* D**65**, 148–155.